The BTK Inhibitor Ibrutinib (PCI-32765) Overcomes Paclitaxel Resistance in ABCB1- and ABCC10-Overexpressing Cells and Tumors

Hui Zhang[#1,2], **Atish Patel**[#1], **Yi-Jun Wang**[1], **Yun-Kai Zhang**[1], **Rishil J. Kathawala**[1], **Long-Hui Qiu**[2], **Bhargav A. Patel**[1], **Li-Hua Huang**[2], **Suneet Shukla**[3], **Dong-Hua Yang**[1], **Suresh V. Ambudkar**[3], **Li-Wu Fu**[2], **Zhe-Sheng Chen**[1]

[1]Department of Pharmaceutical Sciences, College of Pharmacy and Health Sciences, St. John's University, Queens, New York. [2]Sun Yat-Sen University Cancer Center, State Key Laboratory of Oncology in South China, Collaborative Innovation Center for Cancer Medicine, Guangzhou, China. [3]Laboratory of Cell Biology, Center for Cancer Research, National Cancer Institute, NIH, Bethesda, Maryland.

[#] These authors contributed equally to this work.

Abstract

Paclitaxel is one of the most widely used antineoplastic drugs in the clinic. Unfortunately, the occurrence of cellular resistance has limited its efficacy and application. The ATP-binding cassette subfamily B member 1 (ABCB1/P-glycoprotein) and subfamily C member 10 (ABCC10/MRP7) are the major membrane protein transporters responsible for the efflux of paclitaxel, constituting one of the most important mechanisms of paclitaxel resistance. Here, we demonstrated that the Bruton tyrosine kinase inhibitor, ibrutinib, significantly enhanced the antitumor activity of paclitaxel by antagonizing the efflux function of ABCB1 and ABCC10 in cells overexpressing these transporters. Furthermore, we demonstrated that the ABCB1 or ABCC10 protein expression was not altered after treatment with ibrutinib for up to 72 hours using Western blot analysis.

However, the ATPase activity of ABCB1 was significantly stimulated by treatment with ibrutinib. Molecular docking analysis suggested the binding conformation of ibrutinib within the large cavity of the transmembrane region of ABCB1. Importantly, ibrutinib could effectively enhance paclitaxel-induced inhibition on the growth of ABCB1- and ABCC10-overexpressing tumors in nude athymic mice. These results demonstrate that the combination of ibrutinib and paclitaxel can effectively antagonize ABCB1- or ABCC10-mediated paclitaxel resistance that could be of great clinical interest.

Introduction

Paclitaxel, originally isolated from *Taxus brevifolia*, is a drug that stabilizes microtubule dynamics, thus blocking mitotic spindle assembly and cell division (1, 2). Paclitaxel has been used for the treatment of a broad range of cancers, including lung, breast, ovarian, head and neck cancers, and advanced Kaposi sarcoma, leading to increased patient overall survival rate (3, 4). However, the occurrence of drug resistance has been a major limitation to its clinical success. Innate resistance and acquired resistance to paclitaxel is reported to be mediated by multiple mechanisms, such as increased drug efflux, drug inactivation, mutations in the target protein, and evasion of drug-induced damage or apoptosis (5). The drug efflux from cancer cells mediated by ATP-binding cassette subfamily B member 1 (ABCB1/P-gp) and C member 10 (ABCC10/MRP7) is of major concern among the acquired resistance mechanisms to paclitaxel (6, 7). Accumulating evidences from previous studies indicated that overexpression of ABCB1 and ABCC10 are the predominant factors that limit the efficacy of paclitaxel (7–9).

The ABCB1 transporter (also known as P-gp, MDR1) is a 170-kDa full-length ABC transporter membrane glycoprotein, with two transmembrane domains (TMD) and two nucleotide-binding domains (NBD; ref. 10). The ABCB1 transporter can transport a wide range of amphipathic and hydrophobic compounds, such as anthracyclines, taxanes, epipodophyllotoxin derivatives, vinca alkaloids, and derivatives from *Camptotheca acuminate* (6, 10). Overexpression of ABCB1 reduces intracellular drug accumulation and decreases the cytotoxicity of antitumor drugs, thus resulting in multidrug resistance (MDR) and affecting their efficacy (11). The ABCC10 transporter (also known as MRP7) is an important member of MRP subfamily, which is involved in the development of MDR (12). ABCC10, a 171-kDa membrane protein, consists of three TMDs and two NBDs (13). In addition to paclitaxel, ABCC10 has been reported to transport several natural anticancer drugs, including docetaxel, vincristine, vinblastine, vinorelbine, and some synthetic antimetabolites, such as cytarabine, gemcitabine, $2',3'$-dideoxycytidine, 9-(2-phosphonyl methoxyethyl) adenine (PMEA), epothilone B, and endogenous substances like estradiol-17β-D-glucuronide ($E_2$17βG) and leukotriene C4 (9). Hence, there is an increasing demand for novel anticancer agents that can inhibit the function of ABCB1 or ABCC10 and overcome anticancer drug resistance. Previously, we have identified several tyrosine kinase inhibitors (TKI), such as erlotinib (14, 15), nilotinib (16, 17), and lapatinib (14, 18), that have showed a potent effect on overcoming ABCB1- and ABCC10-mediated paclitaxel resistance. Taken together, these reports suggested that TKIs are promising inhibitors of paclitaxel resistance.

Bruton tyrosine kinase (BTK) plays a crucial role in the progression of several B-cell malignancies. Ibrutinib is an effective BTK inhibitor, which has demonstrated promising clinical efficacy in the treatment of various B-cell malignancies (19). The FDA approved ibrutinib for treating patients with mantle cell lymphoma (MCL) and chronic lymphocytic leukemia (CLL; refs. 20, 21). Our previous study demonstrated that ibrutinib effectively overcomes ABCC1-mediated drug resistance (22). However, the effect of ibrutinib on ABCB1- or ABCC10-mediated paclitaxel resistance is still unknown. In this study, we determined whether ibrutinib could significantly enhance the antitumor activity of paclitaxel through inhibiting the efflux function of ABCB1 and ABCC10 both *in vitro* and *in vivo*.

Materials and Methods

Reagents

[^{3}H]-Paclitaxel (37.9 Ci/mmol/L) was purchased from Moravek Biochemicals, Inc. DMEM, FBS, 0.25% trypsin, and penicillin/streptomycin were products of HyClone, Thermo Scientific. Antibody C-219 against ABCB1 was purchased from Signet Laboratories, Inc. Antibodies D-19 against ABCC10 and β-actin were obtained from Santa Cruz Biotechnology, Inc. Ibrutinib was a gift from Johnson & Johnson Services, Inc. Paclitaxel, docetaxel, vincristine, vinblastine, colchicine, cisplatin, and mitoxantrone were purchased from Tocris Bioscience. Cepharanthine was a gift from Kakenshoyaku Co. 3-(4, 5-Dimethylthiazol-yl)-2,5-diphenyltetrazolium bromide (MTT), DMSO, verapamil, and other chemicals were obtained from Sigma Chemical. Fumitremorgin C (FTC) was synthesized by Thomas McCloud Developmental Therapeutics Program, Natural Products Extraction Laboratory (NIH, Bethesda, MD).

Cell lines and cell culture

Human epidermal carcinoma cell line KB-3–1 and colchicine-selected ABCB1-overexpressing cell line KB-C2, the human leukemia cell line K562 and doxorubicin-selected ABCB1-overexpressing derivative cell line K562/AO2 were used in our previous studies (23, 24). Human embryonic kidney cell line HEK293 transfected with empty vector *pcDNA3.1* and *ABCB1*, *ABCC10* stable gene-transfected cell lines, HEK293/ABCB1 and HEK293/ABCC10 were used in all experiments as reported previously (9, 25). *ABCC10* plasmid was from late Dr. Gary D. Kruh's laboratory (University of Illinois at Chicago, Chicago, IL) in January 2011. KB-3–1 and KB-C2 were kindly provided by Dr. Akiyama (Kagoshima University, Kagoshima, Japan). The human leukemia cells K562 and K562/AO2 were from Dr. Chunzheng Yang (Institute of Hematology, Chinese Academy of Medical Sciences, Beijing, China) in May 2013. Cell lines used in this study were thawed from early passage stocks and were passaged for less than 6 months. All the cells were cultured under 37°C, 5% CO$_2$ in DMEM supplemented with 10% heat-inactivated FBS and 1% penicillin/streptomycin. All *in vitro* experiments were conducted at 60% to 80% cell confluence. All the cell lines have been authenticated by authorized organizations.

MTT assay

MTT assay was conducted to measure the sensitivity of the cells to anticancer drugs as described previously (26). The drug concentrations required to inhibit the cell growth by 50% (IC$_{50}$) were calculated from the survival curves.

Immunoblot analysis

To identify whether ibrutinib affects the expression of ABCB1 and ABCC10, the cells were incubated with 5 μmol/L of ibrutinib for 0, 24, 48, and 72 hours. Then, the whole cells were harvested and rinsed twice with ice-cold PBS. Cells were collected with cell lysis buffer (1× PBS, 1% Nonidet P-40, 0.5% sodium deoxycholate, 0.1% SDS, 100 μg/mL phenylmethylsulfonyl fluoride, 10 μg/mL aprotinin, and 10 μg/mL leupeptin). Then, cell lysates were kept on ice for 20 minutes, followed by centrifugation at 10,000 rpm for 15 minutes at 4°C. The supernatant was separated and stored in −80°C until required for the experiment. The protein concentration was quantified using the BCA Assay Kit from Thermo Fischer Scientific Inc. (27). Equal amounts of cell lysate (60 μg) from cells treated with ibrutinib for different time points were resolved by SDS-PAGE and transferred onto polyvinylidene fluoride membranes through electrophoresis. The membrane was then blocked in TBST buffer (10 mmol/L Tris-HCL, 150 mmol/L NaCl, and 0.1% Tween20, pH 8.0) with 5% nonfat milk for 2 hours at room temperature. ABCB1 was determined by C-219 mouse mAb, and ABCC10 was determined by D-19 goat polyclonal antibody. β-Actin was used as an internal loading control as described previously (28).

[³H]-Paclitaxel accumulation assay

The cells were trypsinized, and four aliquots (each 5×10^6 cells) were suspended in the medium. The cells were preincubated with or without ibrutinib (1, 5 μmol/L) or other reversal agents for 1 hour at 37°C. Subsequently, these cells were treated with 0.1 μmol/L [³H]-paclitaxel and incubated further for another 2 hours at 37°C. Then, the suspended cells were pelleted at 4°C and were washed twice with 10 mL ice-cold PBS. The cells were then lysed in 1% SDS, and each sample was placed in the scintillation fluid and radioactivity and was measured using a Packard TRICARB 1900CA liquid scintillation analyzer from Packard Instrument Company Inc. (26).

[³H]-Paclitaxel efflux assay

For the efflux study, the cells were pretreated with or without ibrutinib for 1 hour. The radioactive substrate [³H]-paclitaxel was then added to the cells and further incubated for 2 hours, after which the cells were washed in ice-cold PBS and supplemented with fresh medium with or without ibrutinib at 37°C. After 0, 30, 60, or 120 minutes, the medium of cells was removed and immediately washed twice with 10 mL of ice-cold PBS. The cells were collected and lysed. Each sample was placed in scintillation fluid, and radioactivity was measured as described previously (29).

ABCB1 ATPase assay

The vanadate-sensitive ATPase activity of ABCB1 in crude membranes of High Five insect cells, in the presence of ibrutinib at concentrations ranging from 0 to 80 μmol/L, was measured as described previously (30).

Docking analysis

Ibrutinib structure was built and prepared using protocols for ligand preparation described in our recent report (31). The output file containing at the most 100 unique conformers of ibrutinib was used as an input for docking simulations into the transmembrane-binding site of homology-modeled human ABCB1 (32). The human ABCB1 homology model was prepared following our previous protocols, using the refined mouse ABCB1 crystal structure as the template (32, 33). Docking grid was refined by selecting important residues for drug interaction as reported previously (32). All docking calculations were done using the "Extra Precision" (XP) mode of Glide docking program v6.0 (Schrödinger, LLC, 2013) retaining the default settings. The top-scoring pose of ibrutinib-docked ABCB1 complex structure was then used for graphical analysis. All computations were carried out on a Dell Precision 490n dual processor with Linux OS (Ubuntu 12.04 LTS).

Experimental animals

Male athymic NCR (nu/nu) nude mice (19–24 g, age 5–6 weeks) were purchased from Taconic Farms (NCRNU-M, Homozygous, Albino color) and were used for the ABCB1- and ABCC10-overexpressing tumor xenograft model. Either male or female mice could be used in this study. We conducted the experiments using male mice to make all the conditions of mice consistent. All animals were fed with sterilized food and water and were maintained at the St. John's University Animal Facility. Animals were treated humanely and cared for in accordance with guidelines set forth by the American Association for Accreditation of Laboratory Animal Care and the U.S. Public Health Service Policy on Humane Care and Use of Laboratory Animals. All experiments were carried out in accordance with the guidelines on animal care and experiments of laboratory animals, which were approved by the Institutional Animal Care and Use Committee (IACUC) at St. John's University (Queens, NY), and the research was conducted in compliance with the Animal Welfare Act and other federal statutes.

Nude mouse xenograft model

The ABCB1-overexpressing KB-C2 nude mouse model and ABCC10-overexpressing HEK293/ABCC10 nude mouse model were designed according to our previous studies (9, 34). Briefly, KB-C2 (1.2×10^7) and HEK293/ABCC10 (1.2×10^7) cells were subcutaneously injected under the armpits. When the tumors reached a mean diameter of 5 mm ($n = 7$), the mice were randomized into four groups and treated with one of the following regimens: (a) vehicle [autoclaved water; q3d (every 3 days) × 7]; (b) ibrutinib (30 mg/kg, orally, q3d × 7); (c) paclitaxel (15 mg/kg, i.p., q3d × 7); and (d) ibrutinib (30 mg/kg, orally, q3d × 7) + paclitaxel (15 mg/kg, i.p., q3d × 7) in ABCB1- or ABCC10- overexpressing models. In group (d), the mice were treated with ibrutinib (30 mg/kg, orally) 1 hour before giving paclitaxel. Tumor volumes were measured using calipers and body

weights were recorded (18). The body weight of the animals was monitored every 3 days to adjust the drug dosage and to assess treatment-related toxicities as well as disease progression. The two perpendicular diameters of tumors (termed A and B) were recorded every 3 days, and tumor volume (V) was estimated according to the formula published previously (18).

Statistical analysis

All experiments were repeated at least three times, and the differences were determined using the two-tailed Student t test and statistical significance was determined at $P < 0.05$.

Results

Ibrutinib significantly sensitizes ABCB1- and ABCC10-overexpressing cells to paclitaxel

The MTT assay was performed to determine the cytotoxicity of ibrutinib on the cells used in our study before determining the potential reversal effect of ibrutinib on paclitaxel resistance. As shown in Supplementary Fig. S1, more than 85% of the cells survived with the ibrutinib treatment at the concentration of up to 5 μmol/L. Hence the concentrations of 1, 2.5, and 5 μmol/L were chosen to study the effect of ibrutinib on enhancing the sensitivity of paclitaxel. Our results showed that the nontoxic concentration of ibrutinib significantly increased the cytotoxic effect of paclitaxel in ABCB1-overexpressing KB-C2, K562/AO2 cells and transfected HEK293/ABCB1 cells in a concentration-dependent manner, and the effect is comparable with the well-known inhibitor of ABCB1, verapamil (Table 1). Further studies demonstrated that ibrutinib significantly sensitized ABCC10-overexpressing HEK293/ABCC10 cells to paclitaxel and docetaxel (Table 2). However, ibrutinib showed no enhanced effect of paclitaxel in the KB-3–1, K562, and HEK293/pcDNA3.1, which do not express ABCB1 or ABCC10. Ibrutinib also significantly increased the response of KB-C2, K562/AO2, and HEK293/ABCB1 cells to vincristine and colchicine, which are substrates of ABCB1 (Supplementary Table S1). Similarly, ibrutinib increased the sensitivity of HEK293/ABCC10 cells to vincristine, which is a substrate of ABCC10 (Supplementary Table S2). In addition, ibrutinib did not significantly alter the IC_{50} values of cisplatin, which is not a substrate of ABCB1 or ABCC10 in any of the cell lines. These results suggested that ibrutinib significantly enhance the sensitivity of paclitaxel in MDR cells overexpressing ABCB1 and ABCC10.

Ibrutinib significantly increases the accumulation of [^{3}H]-paclitaxel in MDR cells overexpressing ABCB1 or ABCC10

To understand the potential mechanism of the reversal effect of ibrutinib to paclitaxel resistance in MDR cells, we tested the intracellular accumulation of [^{3}H]-paclitaxel in KB-3–1, KB-C2, HEK293/pcDNA3.1, and HEK293/ABCC10 cells. Our results illustrated that the intracellular [^{3}H]-paclitaxel accumulation was significantly higher in the parental KB-3–1 cells than in the resistant KB-C2 cells. Ibrutinib at 1 and 5 μmol/L significantly increased the intracellular level of [^{3}H]-paclitaxel in KB-C2 cells without affecting the sensitive KB-3–1 cells (Fig. 1A). Similarly, in the presence of 1 and 5 μmol/L of ibrutinib, a significant increase in the intracellular accumulation of [^{3}H]-paclitaxel was observed in HEK293/ABCC10 cells. The effect of ibrutinib at 5 μmol/L was similar to that of

cepharanthine at the same concentration. However, ibrutinib did not alter the intracellular accumulation in the parental HEK293/pcDNA3.1 cells (Fig. 1B). These results indicated that ibrutinib is able to increase the accumulation of [³H]-paclitaxel in the cells overexpressing ABCB1 or ABCC10.

Ibrutinib significantly decreases efflux of [³H]-paclitaxel in MDR cells overexpressing ABCB1 or ABCC10

To determine whether ibrutinib can directly inhibit the efflux activity of ABCB1 and ABCC10, thus leading to the increased intracellular accumulation of [³H]-paclitaxel, we examined the efflux of [³H]-paclitaxel in the presence or absence of ibrutinib at different time points in the MDR cells. Our results indicated that in the absence of ibrutinib, KB-C2 and HEK293/ABCC10 cells efflux more [³H]-paclitaxel out of the cells comparing with their paired sensitive cells, KB-3–1 and HEK293/pcDNA3.1 cells at different time points. However, the efflux activities of ABCB1 and ABCC10 were significantly inhibited with the treatment of 5 μmol/L of ibrutinib at 30, 60, and 120 minutes, thus inducing an increased accumulation of [³H]-paclitaxel in the MDR cells but not in the parental sensitive cells (Fig. 1C and D). These results further validated the efficacy of ibrutinib to inhibit the drug efflux function of ABCB1 and ABCC10.

Ibrutinib does not significantly alter the protein expression of ABCB1 or ABCC10 in the MDR cells

The reversal effect of ibrutinib might act by either inhibiting the function of the protein or decreasing the expression of the protein. To ascertain whether ibrutinib affects the protein expression of ABCB1 and ABCC10, we treated the MDR cells with 5 μmol/L of ibrutinib for 24, 48, and 72 hours. Immunoblot analysis confirmed that ibrutinib did not significantly alter the protein expression of ABCB1 or ABCC10 in the MDR cells (Fig. 2A and B). These findings suggested that the reversal of paclitaxel resistance by ibrutinib is not the result of decreased ABCB1 or ABCC10 protein expression.

Ibrutinib stimulates the ATPase activity of ABCB1

The drug efflux process by ABC transporters utilizes the energy from hydrolysis of ATP to ADP to transport their substrates. Substrates or modulators that interact with the transporter might stimulate or inhibit ATPase activity. To assess the effect of ibrutinib on the ATPase activity of ABCB1, we tested ABCB1-mediated ATP hydrolysis with different concentrations of ibrutinib (0–80 μmol/L). Ibrutinib stimulated the ATPase activity of ABCB1 in a concentration-dependent manner, with a maximal stimulation of 3.05-fold of the basal activity. Figure 2C demonstrates that the concentration of ibrutinib required to obtain 50% stimulation is 0.641 μmol/L. The results suggested that ibrutinib interacts with ABCB1 transporter in a substrate manner.

Molecular docking analysis of ibrutinib with human ABCB1 homology model

In the absence of the crystal structure of human ABCB1, we developed a homology model based on the updated crystal structure of ABCB1 from mice (32). To understand the molecular interactions of ibrutinib with human ABCB1, docking studies were performed

within the drug-binding cavity of homology-modeled human ABCB1. The top docking score was found to be −9.6 kcal/mol, and we used this pose for discussion of the binding interactions within the large binding site in ABCB1 (35). The figure of ibrutinib and nearby residues is shown in Fig. 2D.

The docking pose indicated the importance of hydrophobic and electrostatic interactions within the large drug-binding cavity of ABCB1. The two-benzene group (D- and E-ring) forms hydrophobic contacts with side chains of residues Ile306, Leu339, Phe343, and Gln990. The pyrazole and pyrimidine ring (B- and C-ring) bind to the hydrophobic pocket formed by the side chains of residue Tyr310, Phe728, Ala729, Phe732, and Phe983. Moreover, the piperidine (A-ring) is stabilized by hydrophobic contact with Met69, Phe335, Phe336, Ile340, Tyr953, and Phe983. In addition, N_3 atom of C-ring formed a hydrogen bonding interaction with side chain amide "NH" of Gln725 (–N⋯H_2N-Gln725, 1.78 Å). The carbonyl oxygen atom in Gln725 also formed a hydrogen bond with the amino group in C-ring (-NH-H⋯OC-Gln725, 2.07 Å).

Ibrutinib significantly potentiates the anticancer activity of paclitaxel in ABCB1- and ABCC10-overexpressing cell xenograft mouse models

An established KB-C2 cell xenograft model in nude mice was used to evaluate the efficacy of ibrutinib on paclitaxel-induced antitumor activity. After a series of pilot studies, we selected a dose of 30 mg/kg of ibrutinib and 15 mg/kg of paclitaxel in the studies. As shown in Fig. 3A, there was no significant difference in tumor size between groups treated with saline and ibrutinib. The group treated with paclitaxel (15 mg/kg i.p.) mildly reduced the growth rate of tumors compared with saline control group. However, the group treated with ibrutinib (30 mg/kg orally, given 1 hour before giving paclitaxel) in combination with paclitaxel (15 mg/kg i.p.) produced a significant inhibition of tumor growth compared with groups treated with saline, paclitaxel, or ibrutinib alone (Fig. 3A and B). The mean values of the weight of tumors removed from sacrificed mice were analyzed in Fig. 3C. In addition, there was no significant difference in body weight or in phenotypic changes between the treatment groups after the course of therapy (Fig. 3D). Our results suggested that ibrutinib (30 mg/kg orally, given 1 hour before giving paclitaxel) in combination with paclitaxel improve the antitumor efficacy of paclitaxel in KB-C2 cell xenograft model without increasing toxicity. Similarly, we established an HEK293/ABCC10 cell xenograft model in nude mice that was used to evaluate the efficacy of ibrutinib on paclitaxel-induced antitumor activity. Our results demonstrated that the combination of ibrutinib and paclitaxel produced a significant inhibition of tumor growth compared with mice treated with paclitaxel, saline, or ibrutinib alone ($P < 0.05$; Fig. 4A–C). Furthermore, at the selected doses, no mortality or apparent decrease in body weight was observed in all the groups, suggesting that the combination regimen does not increase the incidence of toxic side effects (Fig. 4D).

Discussion

Paclitaxel has been widely used alone or in combined regiments and has shown prominent effect on treating patients with lung, ovarian, breast, head and neck cancers, and advanced forms of Kaposi sarcoma (36). However, the occurrence of MDR limited the clinical

efficacy. As reported previously, overexpression of ABCB1 is one of the most prominent mechanisms underlying paclitaxel resistance (37). Recently, ABCC10 was proved to be another important factor for the occurrence of paclitaxel resistance (38, 39). Ibrutinib has shown promising activity for the treatment of relapsed or refractory MCL and CLL and been approved by the FDA (40). In addition, ibrutinib demonstrated potent antitumor activity in EGFR-mutant non–small cell lung cancer (41). Our previous report found that ibrutinib was a potent inhibitor of MRP1 (22). However, no data are available on whether ibrutinib could enhance the efficacy of paclitaxel and other drugs that are the substrates of ABCB1 or ABCC10 transporter. Therefore, this preclinical study using the combination of ibrutinib with paclitaxel would be of great clinical interest.

The cytotoxicity of ibrutinib on cells used in our study was investigated and found nontoxic at the concentrations of 1, 2.5, and 5 μmol/L. The concentration of 5 μmol/L was used to study its potential mechanisms to reverse paclitaxel resistance. We found that ibrutinib significantly potentiated the cytotoxicity of paclitaxel in KB-C2, HEK293/ABCB1, and K562/AO2 cells that overexpress ABCB1 in a concentration-dependent manner. Further studies showed that ibrutinib significantly enhanced the cytotoxicity of paclitaxel in HEK293/ABCC10 cells. In addition, ibrutinib also potentiated the cytotoxicity of other substrates of ABCB1 or ABCC10 but not cisplatin, which is not a substrate of these two transporters. However, ibrutinib showed no significant effect on the parental KB-3–1, k562, and HEK293/pcDNA3.1 cells. Moreover, ibrutinib did not enhance the sensitivity of the ABCG2 substrate mitoxantrone on ABCG2-overexpressing cells (Supplementary Table S3). These findings indicated that ibrutinib may antagonize ABCB1- and ABCC10-mediated paclitaxel resistance. We also confirmed that this effect was due to a significant increase in the intracellular accumulation of [^{3}H]-paclitaxel in the resistant cells. Consistent with the previous results, [^{3}H]-paclitaxel efflux experiments showed that ibrutinib significantly reduced the rapid efflux of the [^{3}H]-paclitaxel in KB-C2 and HEK293/ABCC10 cells in a time-dependent manner.

The effect of ibrutinib on ABCB1- and ABCC10-mediated paclitaxel resistance could be either by antagonizing the function of the transporters or lowering the protein expression levels. We performed Western blot analysis to analyze the expression of ABCB1 and ABCC10 after incubating the cells with ibrutinib for 24, 48, and 72 hours. Western blot results illustrated that ibrutinib did not alter the expression of ABCB1 or ABCC10 when the cells were incubated with ibrutinib for up to 72 hours. This excludes the possibility that the effect of ibrutinib on paclitaxel resistance was due to alteration of the protein expression.

Because the ABC transporters utilize energy derived from ATP hydrolysis to pump the substrate drugs out of the cells, the profile of drug-stimulated ATPase activity in the ABCB1-expressing cell membrane is considered to reflect the interaction of transporter pumps with drug substrates (42). Thus ATPase assay was performed to test the interaction of ibrutinib and ABCB1 transporter. Ibrutinib was found to stimulate ATPase activity in a concentration-dependent manner, suggesting that ibrutinib may be a substrate and therefore a competitive inhibitor of ABCB1. In addition, we performed molecular docking analysis and identified the binding conformation of ibrutinib within the large cavity of the transmembrane region of ABCB1.

To examine whether ibrutinib can also reverse ABCB1- and ABCC10-mediated paclitaxel resistance *in vivo*, the effects of ibrutinib on the toxicity of paclitaxel in the nude mouse xenograft models were studied. Previous pharmacokinetics study of ibrutinib in mice showed its peak plasma concentration of 1.07 μmol/L when the mice were administered a 14.2 mg/kg dose (43). In addition, our *in vitro* results suggested that the concentration of ibrutinib between 1 and 5 μmol/L significantly overcame paclitaxel resistance. Therefore, the peak of plasma concentration must be greater than 1.07 μmol/L when the mice were administered a 30 mg/kg dose of ibrutinib. On the basis of this, we chose 30 mg/kg to conduct pilot experiments. The results showed that ibrutinib at 30 mg/kg did not produce any visible toxicity or phenotypic changes in the mice. Therefore, 30 mg/kg was chosen in *in vivo* studies. The intraperitoneal dose of paclitaxel (15 mg/kg) used in this study was determined according to the results of our previous study, which indicated that it produced significant resistance in HEK293/ABCC10 tumor xenograft model compared with the HEK293/pcDNA3.1 tumor xenograft model (39). Consistent with *in vitro* experiments, the results obtained from *in vivo* studies showed that the combination of paclitaxel with ibrutinib enhanced the anticancer activity of paclitaxel in the ABCB1- and ABCC10-overexpressing xenograft mouse models.

Clinical studies have also implied the interactions between ibrutinib and some chemotherapeutics that are substrates of ABC transporters. For the treatment of non-Hodgkin lymphoma, ibrutinib showed synergistic effect when combined with cyclophosphamide, doxorubicin, and vincristine, that are substrates of MRP1 (44). In another phase II trial, the combination of ibrutinib and MRP1 substrate bendamustine demonstrated synergistic effect in relapsed and refractory CLL (45). In our study, the combination of ibrutinib and paclitaxel demonstrated strong synergistic effect, most likely due to the inhibitory function of ibrutinib on both ABCB1 and ABCC10, leading to reducing the efflux of paclitaxel by ABCB1 and ABCC10. This synergy was demonstrated across a large panel of cell lines, including those representing human leukemia and some solid tumors. In addition, the KB-C2 and HEK293/ABCC10 nude mouse models confirmed the therapeutic benefits of the combination treatment *in vivo*.

Collectively, our results suggested that ibrutinib has previously unknown function in sensitizing ABCB1- or ABCC10- overexpressing cells to the substrate paclitaxel both *in vitro* and *in vivo*. This effect was most likely due to the blockage of the efflux of paclitaxel by ABCB1 or ABCC10. Therefore, the combination therapy of ibrutinib and paclitaxel could represent an efficient strategy to treat patients with cancers that are resistant to paclitaxel as a result of the expression of ABCB1 or ABCC10.

Supplementary Material

Refer to Web version on PubMed Central for supplementary material.

Acknowledgments

References

1. Jordan MA, Wilson L. Microtubules as a target for anticancer drugs. Nat Rev Cancer 2004;4:253–65. [PubMed: 15057285]

2. Rowinsky EK, Donehower RC. Paclitaxel (taxol). N Engl J Med 1995;332: 1004–14. [PubMed: 7885406]

3. Whelan J Targeted taxane therapy for cancer. Drug Discov Today 2002; 7:90–2. [PubMed: 11790612]

4. Choong NW, Vokes EE, Haraf DJ, Tothy PK, Ferguson MK, Kasza K, et al. Phase I study of induction chemotherapy and concomitant chemoradiotherapy with irinotecan, carboplatin, and paclitaxel for stage III non-small cell lung cancer. J Thorac Oncol 2008;3:59–67. [PubMed: 18166842]

5. Perez EA. Microtubule inhibitors: Differentiating tubulin-inhibiting agents based on mechanisms of action, clinical activity, and resistance. Mol Cancer Ther 2009;8:2086–95. [PubMed: 19671735]

6. Szakacs G, Paterson JK, Ludwig JA, Booth-Genthe C, Gottesman MM. Targeting multidrug resistance in cancer. Nat Rev Drug Discov 2006; 5:219–34. [PubMed: 16518375]

7. Duan Z, Brakora KA, Seiden MV. Inhibition of ABCB1 (MDR1) and ABCB4 (MDR3) expression by small interfering RNA and reversal of paclitaxel resistance in human ovarian cancer cells. Mol Cancer Ther 2004;3:833–8. [PubMed: 15252144]

8. Mickisch GH, Merlino GT, Galski H, Gottesman MM, Pastan I. Transgenic mice that express the human multidrug-resistance gene in bone marrow enable a rapid identification of agents that reverse drug resistance. Proc Natl Acad Sci U S A 1991;88:547–51. [PubMed: 1671173]

9. Kathawala RJ, Sodani K, Chen K, Patel AS, Abuznait AH, Anreddy N, et al. Masitinib antagonizes ATP-binding cassette subfamily C member 10-mediated paclitaxel resistance: a preclinical study. Mol Cancer Ther 2014; 13:714–23. [PubMed: 24431074]

10. Sharom FJ. ABC multidrug transporters: structure, function and role in chemoresistance. Pharmacogenomics 2008;9:105–27. [PubMed: 18154452]

11. Gottesman MM, Pastan I, Ambudkar SV. P-glycoprotein and multidrug resistance. Curr Opin Genet Dev 1996;6:610–7. [PubMed: 8939727]

12. Kathawala RJ, Wang YJ, Ashby CR Jr, Chen ZS. Recent advances regarding the role of ABC subfamily C member 10 (ABCC10) in the efflux of antitumor drugs. Chin J Cancer 2014;33:223–30. [PubMed: 24103790]

13. Chen ZS, Hopper-Borge E, Belinsky MG, Shchaveleva I, Kotova E, Kruh GD. Characterization of the transport properties of human multidrug resistance protein 7 (MRP7, ABCC10). Mol Pharmacol 2003;63:351–8. [PubMed: 12527806]

14. Kuang YH, Shen T, Chen X, Sodani K, Hopper-Borge E, Tiwari AK, et al. Lapatinib and erlotinib are potent reversal agents for MRP7 (ABCC10)-mediated multidrug resistance. Biochem Pharmacol 2010;79:154–61. [PubMed: 19720054]

15. Shi Z, Peng XX, Kim IW, Shukla S, Si QS, Robey RW, et al. Erlotinib (Tarceva, OSI-774) antagonizes ATP-binding cassette subfamily B member 1 and ATP-binding cassette subfamily G member 2-mediated drug resistance. Cancer Res 2007;67:11012–20. [PubMed: 18006847]

16. Tiwari AK, Sodani K, Wang SR, Kuang YH, Ashby CR Jr, Chen X, et al. Nilotinib (AMN107, Tasigna) reverses multidrug resistance by inhibiting the activity of the ABCB1/Pgp and ABCG2/BCRP/MXR transporters. Biochem Pharmacol 2009;78:153–61. [PubMed: 19427995]

17. Shen T, Kuang YH, Ashby CR, Lei Y, Chen A, Zhou Y, et al. Imatinib and nilotinib reverse multidrug resistance in cancer cells by inhibiting the efflux activity of the MRP7 (ABCC10). PLoS One 2009;4:e7520. [PubMed: 19841739]

18. Dai CL, Tiwari AK, Wu CP, Su XD, Wang SR, Liu DG, et al. Lapatinib (Tykerb, GW572016) reverses multidrug resistance in cancer cells by inhibiting the activity of ATP-binding cassette subfamily B member 1 and G member 2. Cancer Res 2008;68:7905–14. [PubMed: 18829547]

19. Cheng S, Ma J, Guo A, Lu P, Leonard JP, Coleman M, et al. BTK inhibition targets *in vivo* CLL proliferation through its effects on B-cell receptor signaling activity. Leukemia 2014;28:649–57. [PubMed: 24270740]

20. Ibrutinib approved for mantle cell lymphoma. Cancer Discov 2014;4:OF1.

21. Ibrutinib (Imbruvica) for chronic lymphocytic leukemia. Med Lett Drugs Ther 2014;56:29–30. [PubMed: 24736247]

22. Zhang H, Patel A, Ma SL, Li XJ, Zhang YK, Yang PQ, et al. *In vitro*, *in vivo* and ex-vivo characterization of ibrutinib: a potent inhibitor of MRP1 efflux function. Br J Pharmacol 2014;171:5845–57. [PubMed: 25164592]

23. Akiyama S, Seth P, Pirker R, FitzGerald D, Gottesman MM, Pastan I. Potentiation of cytotoxic activity of immunotoxins on cultured human cells. Cancer Res 1985;45:1005–7. [PubMed: 2982480]

24. Ichikawa Y, Hirokawa M, Aiba N, Fujishima N, Komatsuda A, Saitoh H, et al. Monitoring the expression profiles of doxorubicin-resistant K562 human leukemia cells by serial analysis of gene expression. Int J Hematol 2004;79:276–82. [PubMed: 15168598]

25. Robey RW, Shukla S, Finley EM, Oldham RK, Barnett D, Ambudkar SV, et al. Inhibition of P-glycoprotein (ABCB1)- and multidrug resistance-associated protein 1 (ABCC1)-mediated transport by the orally administered inhibitor, CBT-1((R)). Biochem Pharmacol 2008;75:1302–12. [PubMed: 18234154]

26. Patel A, Tiwari AK, Chufan EE, Sodani K, Anreddy N, Singh S, et al. PD173074, a selective FGFR inhibitor, reverses ABCB1-mediated drug resistance in cancer cells. Cancer Chemother Pharmacol 2013;72:189–99. [PubMed: 23673445]

27. Ding PR, Tiwari AK, Ohnuma S, Lee JW, An X, Dai CL, et al. The phosphodiesterase-5 inhibitor vardenafil is a potent inhibitor of ABCB1/P-glycoprotein transporter. PLoS One 2011;6:e19329. [PubMed: 21552528]

28. Zhang H, Wang YJ, Zhang YK, Wang DS, Kathawala RJ, Patel A, et al. AST1306, a potent EGFR inhibitor, antagonizes ATP-binding cassette subfamily G member 2-mediated multidrug resistance. Cancer Lett 2014; 350:61–8. [PubMed: 24747122]

29. Yang D, Kathawala RJ, Chufan EE, Patel A, Ambudkar SV, Chen ZS, et al. Tivozanib reverses multidrug resistance mediated by ABCB1 (P-glycoprotein) and ABCG2 (BCRP). Future Oncol 2014;10:1827–41. [PubMed: 24295377]

30. Ambudkar SV. Drug-stimulatable ATPase activity in crude membranes of human MDR1-transfected mammalian cells. Methods Enzymol 1998; 292:504–14. [PubMed: 9711578]

31. Guo HQ, Zhang GN, Wang YJ, Zhang YK, Sodani K, Talele TT, et al. beta-Elemene, a compound derived from Rhizoma zedoariae, reverses multidrug resistance mediated by the ABCB1 transporter. Oncol Rep 2014;31: 858–66. [PubMed: 24284783]

32. Li J, Jaimes KF, Aller SG. Refined structures of mouse P-glycoprotein. Protein Sci 2014;23:34–46. [PubMed: 24155053]

33. Singh S, Prasad NR, Chufan EE, Patel BA, Wang YJ, Chen ZS, et al. Design and synthesis of human ABCB1 (P-Glycoprotein) inhibitors by peptide coupling of diverse chemical scaffolds on carboxyl and amino termini of (S)-valine-derived thiazole amino acid. J Med Chem 2014;57:4058–72. [PubMed: 24773054]

34. Tiwari AK, Sodani K, Dai CL, Abuznait AH, Singh S, Xiao ZJ, et al. Nilotinib potentiates anticancer drug sensitivity in murine ABCB1-, ABCG2-, and ABCC10-multidrug resistance xenograft models. Cancer Lett 2013;328: 307–17. [PubMed: 23063650]

35. Ferreira RJ, Ferreira MJ, Dos Santos DJ. Molecular Docking characterizes substrate-binding sites and efflux modulation mechanisms within P-Glycoprotein. J Chem Informat Model 2013;53:1747–60.

36. Wani MC, Taylor HL, Wall ME, Coggon P, McPhail AT. Plant antitumor agents. VI. The isolation and structure of taxol, a novel antileukemic and antitumor agent from Taxus brevifolia. J Am Chem Soc 1971; 93:2325–7. [PubMed: 5553076]

37. Stordal B, Davey R. A systematic review of genes involved in the inverse resistance relationship between cisplatin and paclitaxel chemotherapy: role of BRCA1. Curr Cancer Drug Targets 2009;9:354–65. [PubMed: 19442054]

38. Sodani K, Patel A, Kathawala RJ, Chen ZS. Multidrug resistance associated proteins in multidrug resistance. Chin J Cancer 2012;31:58–72. [PubMed: 22098952]

39. Kathawala RJ, Sodani K, Chen K, Patel A, Abuznait AH, Anreddy N, et al. Masitinib antagonizes ATP-binding cassette subfamily C member 10-mediated paclitaxel resistance: a preclinical study. Mol Cancer Ther 2014;13:714–23. [PubMed: 24431074]

40. Tang R, Faussat AM, Majdak P, Perrot JY, Chaoui D, Legrand O, et al. Valproic acid inhibits proliferation and induces apoptosis in acute myeloid leukemia cells expressing P-gp and MRP1. Leukemia 2004;18:1246–51. [PubMed: 15116123]

41. Gao W, Wang M, Wang L, Lu H, Wu S, Dai B, et al. Selective antitumor activity of ibrutinib in EGFR-mutant non-small cell lung cancer cells. J Natl Cancer Inst 2014;106:dju204. [PubMed: 25214559]

42. Cole SP, Bhardwaj G, Gerlach JH, Mackie JE, Grant CE, Almquist KC, et al. Overexpression of a transporter gene in a multidrug-resistant human lung cancer cell line. Science 1992;258:1650–4. [PubMed: 1360704]

43. Honigberg LA, Smith AM, Sirisawad M, Verner E, Loury D, Chang B, et al. The Bruton tyrosine kinase inhibitor PCI-32765 blocks B-cell activation and is efficacious in models of autoimmune disease and B-cell malignancy. Proc Natl Acad Sci USA 2010;107:13075–80. [PubMed: 20615965]

44. Younes A, Thieblemont C, Morschhauser F, Flinn I, Friedberg JW, Amorim S, et al. Combination of ibrutinib with rituximab, cyclophosphamide, doxorubicin, vincristine, and prednisone (R-CHOP) for treatment-naive patients with CD20-positive B-cell non-Hodgkin lymphoma: a non-randomised, phase 1b study. Lancet Oncol 2014;15:1019–26. [PubMed: 25042202]

45. Fischer K, Cramer P, Busch R, Stilgenbauer S, Bahlo J, Schweighofer CD, et al. Bendamustine combined with rituximab in patients with relapsed and/or refractory chronic lymphocytic leukemia: a multicenter phase II trial of the German Chronic Lymphocytic Leukemia Study Group. J Clin Oncol 2011;29:3559–66. [PubMed: 21844497]
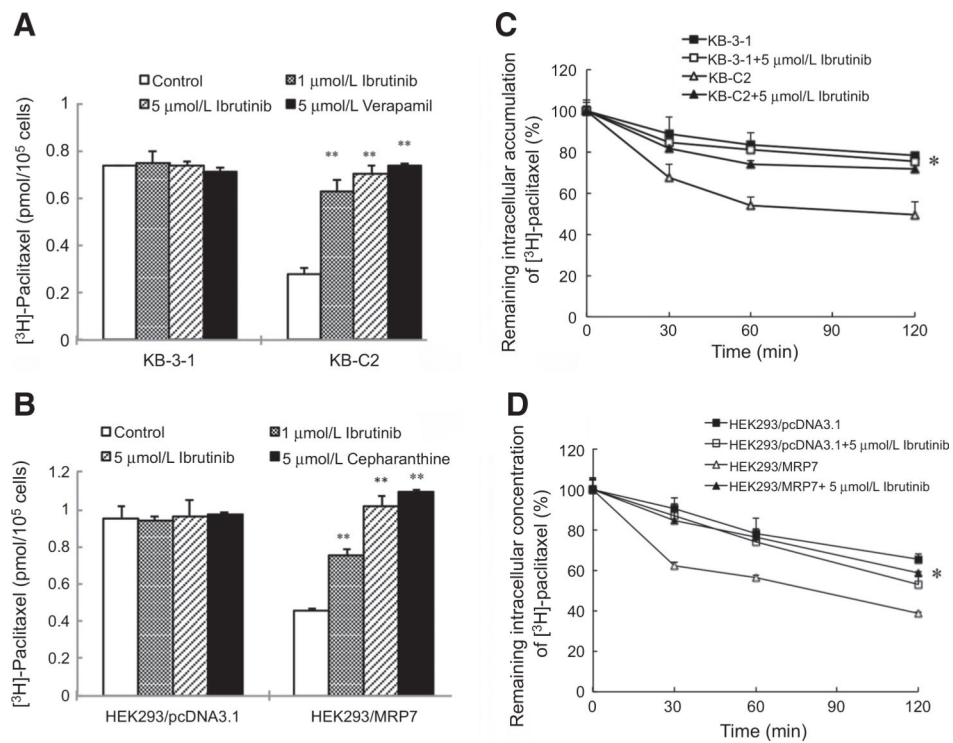
Figure 1.
The effect of ibrutinib on the accumulation and efflux of [^{3}H]-paclitaxel in ABCB1- or ABCC10-overexpressing cells. **A,** Ibrutinib effectively increased the accumulation of [^{3}H]-paclitaxel in KB-C2 cells. Columns are the mean of triplicate determinations; bars, SDs. **B,** The efficacy of ibrutinib on the efflux of [^{3}H]-paclitaxel from KB-3–1 and KB-C2 cells was measured. A time-dependent versus percentage of intracellular [^{3}H]-paclitaxel was plotted (0, 30, 60, and 120 minutes). Data shown were means ± SDs for independent determinations in triplicate. **C,** Ibrutinib effectively increased the accumulation of [^{3}H]-paclitaxel in HEK293/ABCC10 cells. **D,** The effect of ibrutinib on the efflux of [^{3}H]-paclitaxel from HEK293/pcDNA3.1 and HEK293/ABCC10 cells was measured. Three independent experiments were performed.
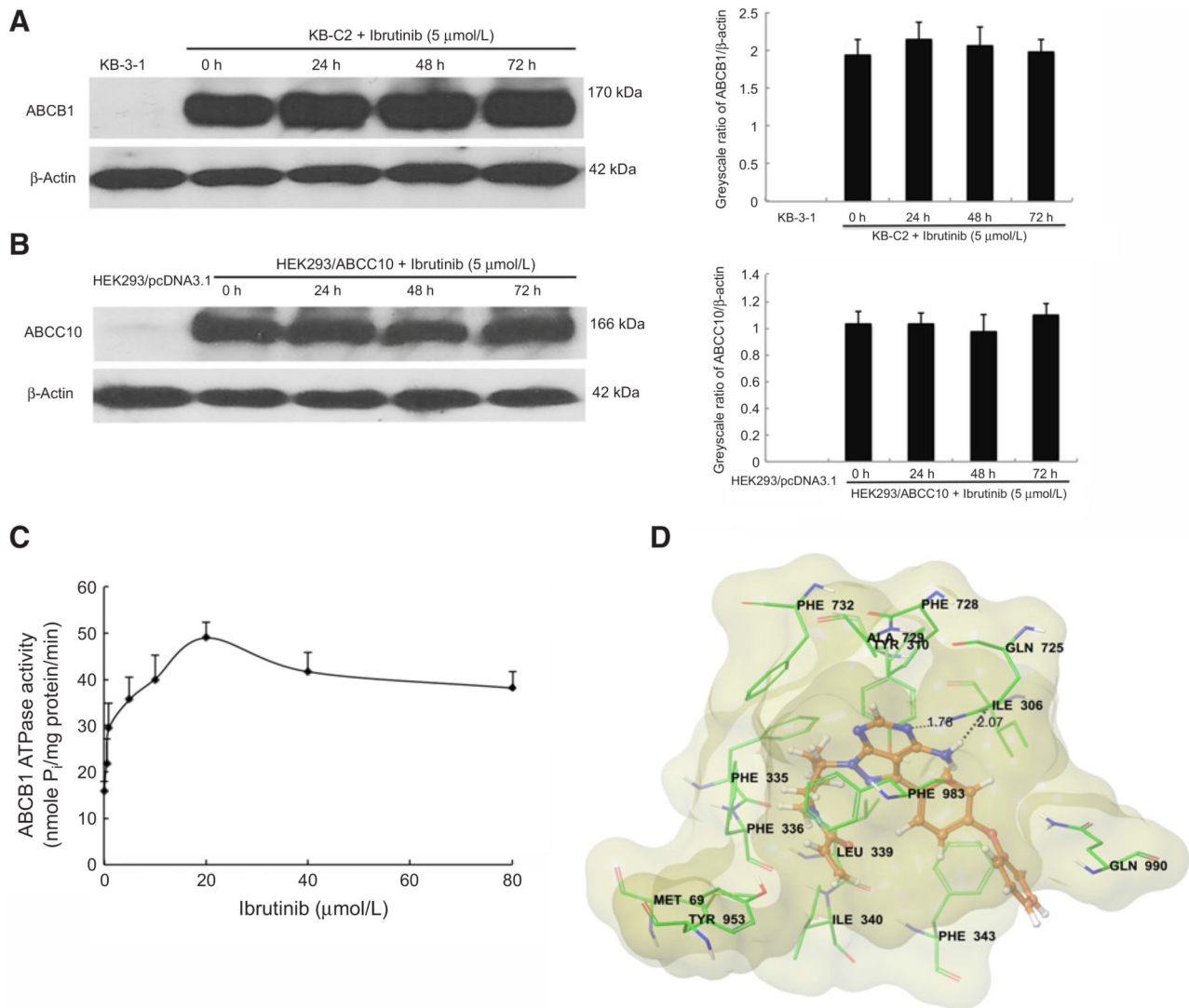
Figure 2.
The effect of ibrutinib on ABCB1 and ABCC10 expression levels, ABCB1 ATPase activity, and its docking in the homology model of ABCB1. **A,** The effect of ibrutinib on the protein levels of ABCB1 was tested by Western blot analysis after the KB-C2 cells were treated with 5 μmol/L ibrutinib for 0, 24, 48, and 72 hours. The expression levels of ABCB1 were normalized by β-actin. The differences were statistically not significant ($P > 0.05$). **B,** The effect of ibrutinib on the protein levels of ABCC10; the expression levels of ABCC10 were normalized by β-actin. **C,** The effect of ibrutinib (0–80 μmol/L) on ATP hydrolysis by ABCB1. The mean values are plotted, and error bars represent the SD. The experiments were performed at least three independent times. **D,** XP-Glide predicted binding mode of ibrutinib with homology-modeled ABCB1. The docked conformation of ibrutinib as ball and stick model is shown within the large hydrophobic cavity of ABCB1. Important amino acids are depicted as sticks with the atoms colored as carbon, green; hydrogen, white; nitrogen, blue; oxygen, red; sulfur, yellow, whereas ibrutinib is shown with the same color scheme as above except carbon atoms are represented in orange. Dotted black line, hydrogen bonding

interactions. Molecular surface of homology-modeled ABCB1 was colored by residue charge (hydrophobic, yellow).

Figure 3.
Ibrutinib enhanced the effect of paclitaxel on the growth of an ABCB1-overexpressing KB-C2 cell xenograft model in athymic nude mice. **A,** Images of excised KB-C2 tumor tissues from different mice are shown on the 18th day after treatment ($n = 7$). **B,** Changes in tumor volume with time in ABCB1-overexpressing xenograft model are shown. **C,** Mean weight ($n = 7$) of the excised KB-C2 tumors from the mice treated with vehicle, ibrutinib, paclitaxel, or the combination of ibrutinib and paclitaxel. Error bars, SD. *, $P < 0.05$ versus vehicle group; #, $P < 0.05$ versus the paclitaxel group. **D,** The average body weight before and after treatments.
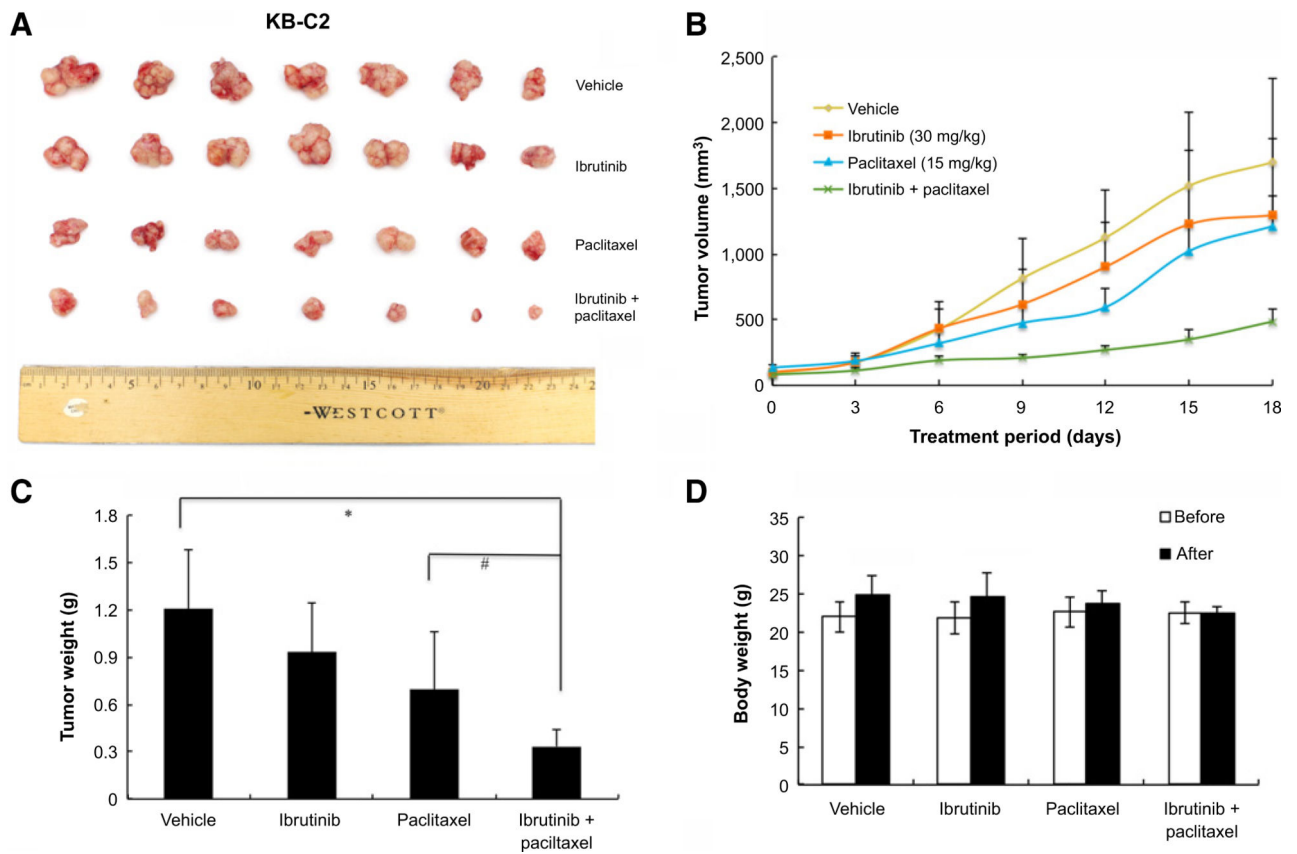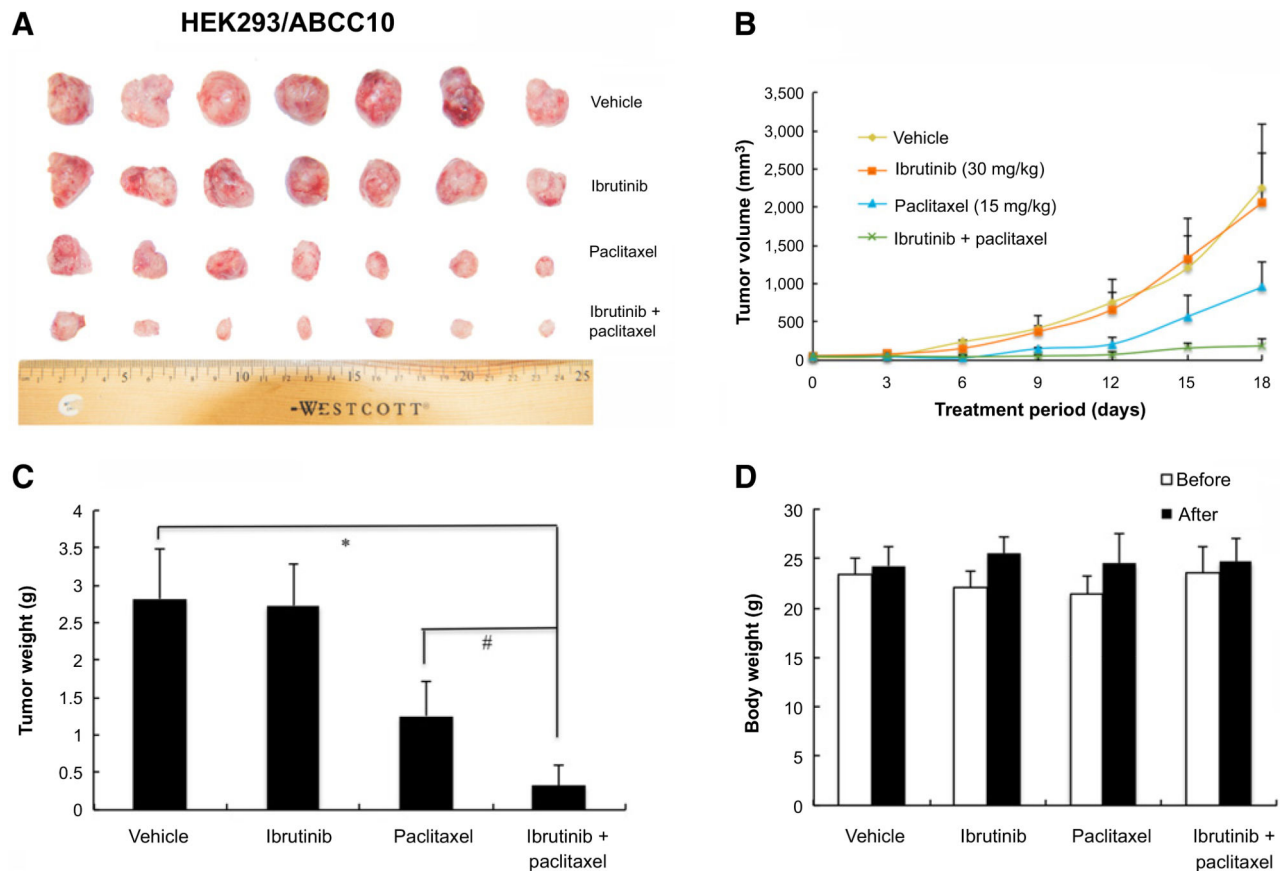
Figure 4.
Ibrutinib enhanced the effect of paclitaxel on the growth of an ABCC10-overexpressing HEK293/ABCC10 cell xenograft model in athymic nude mice. **A,** Images of excised HEK293/ABCC10 tumors tissues from different mice are shown on the 18th day after treatment ($n = 7$). **B,** Changes in tumor volume with time in ABCC10-overexpressing xenograft model are shown. **C,** Mean weight ($n = 7$) of the excised HEK293/ABCC10 tumors from the mice treated with vehicle, ibrutinib, paclitaxel, or the combination of ibrutinib and paclitaxel. Error bars, SD. *, $P < 0.05$ versus vehicle group; #, $P < 0.05$ versus the paclitaxel group. **D,** The average body weight before and after treatments.

Table 1.

Ibrutinib enhances the effect of paclitaxel in ABCB1-overexpressing cells

Drugs	$IC_{50} \pm SD^a$ (nmol/L; fold resistance)	
	KB-3-1	**KB-C2**
Paclitaxel	0.35 ± 0.02 $(1.00)^b$	38.91 ± 1.86 (111.17)
+Ibrutinib 1 μmol/L	0.37 ± 0.05 (1.05)	7.65 ± 0.92 $(21.71)^c$
+Ibrutinib 2.5 μmol/L	0.36 ± 0.06 (1.03)	3.19 ± 0.53 $(6.02)^c$
+Ibrutinib 5 μmol/L	0.38 ± 0.07 (1.09)	0.91 ± 0.08 $(2.6)^c$
+Verapamil 5 μmol/L	0.34 ± 0.03 (0.97)	1.18 ± 0.19 $(3.37)^c$
Cisplatin	$2,709.79 \pm 226.25$ $(1.00)^b$	$2,276.11 \pm 213.81$ (0.84)
+Ibrutinib 1 μmol/L	$2,601.54 \pm 331.01$ (0.96)	$2,258.57 \pm 195.83$ (0.83)
+Ibrutinib 2.5 μmol/L	$2,507.75 \pm 197.13$ (0.93)	$2,251.71 \pm 287.17$ (0.83)
+Ibrutinib 5 μmol/L	$2,542.87 \pm 231.55$ (0.94)	$2,306.39 \pm 248.05$ (0.85)
+Verapamil 5 μmol/L	$2,721.24 \pm 274.60$ (1.00)	$2,358.20 \pm 148.95$ (0.87)
	K562	**K562/AO2**
Paclitaxel	5.08 ± 0.62 (1.00)	820.59 ± 71.03 (161.53)
+Ibrutinib (1 μmol/L)	4.64 ± 0.59 (0.91)	515.33 ± 66.21 $(101.44)^c$
+Ibrutinib (2.5 μmol/L)	4.74 ± 0.87 (0.93)	184.67 ± 20.33 $(36.35)^c$
+Verapamil (2.5 μmol/L)	4.80 ± 0.48 (0.94)	141.36 ± 18.91 $(25.85)^c$
Cisplatin	$4,188.82 \pm 400.43$ (1.00)	$4,974.80 \pm 400.32$ (1.19)
+Ibrutinib (1 μmol/L)	$4,185.74 \pm 200.05$ (1.00)	$4,373.33 \pm 698.68$ (1.04)
+Ibrutinib (2.5 μmol/L)	$4,815.90 \pm 759.21$ (1.15)	$4,582.47 \pm 600.09$ (1.09)
+Verapamil (2.5 μmol/L)	$4,296.62 \pm 459.60$ (1.03)	$5,167.82 \pm 600.31$ (1.23)
	HEK293/pcDNA3.1	**HEK293/ABCB1**
Paclitaxel	3.24 ± 0.51 $(1.00)^b$	545.00 ± 20.21 (168.21)
+Ibrutinib 1 μmol/L	2.93 ± 0.41 (0.90)	291.26 ± 31.39 $(89.90)^c$
+Ibrutinib 2.5 μmol/L	3.07 ± 0.65 (0.95)	99.42 ± 11.44 $(30.69)^c$

| Drugs | IC$_{50}$ ± SD[a] (nmol/L; fold resistance) | |
	KB-3-1	KB-C2
+Ibrutinib 5 μmol/L	2.97 ± 0.53 (0.92)	8.79 ± 1.76 (2.70)[c]
+Verapamil 5 μmol/L	3.05 ± 0.39 (0.94)	6.44 ± 1.23 (1.99)[c]
Cisplatin	1,308.24 ± 132.33 (1.00)[b]	1,142.00 ± 61.28 (0.87)
+Ibrutinib 1 μmol/L	1,320.33 ± 146.49 (1.01)	1,071.76 ± 36.89 (0.82)
+Ibrutinib 2.5 μmol/L	1,369.42 ± 175.93 (1.05)	1,211.95 ± 193.30 (0.93)
+Ibrutinib 5 μmol/L	1,310.45 ± 128.63 (1.00)	1,172.69 ± 147.66 (0.90)
+Verapamil 5 μmol/L	1,260.24 ± 96.82 (0.96)	1,236.06 ± 170.06 (0.94)

NOTE: Cell survival was determined by MTT.

[a] Values represent IC$_{50}$ ± SD of at least three independent experiments performed in triplicate.

[b] The fold reversal of MDR (values given in parentheses) was calculated by dividing the IC$_{50}$ values of substrate in the resistant cells in the absence or presence of inhibitors, or the parent cells with inhibitors, by the IC$_{50}$ of the parental cells without reversal agents.

[c] $P < 0.05$, significantly different from values obtained in the absence of the reversal agents.

Table 2.

Ibrutinib enhances the effect of paclitaxel and docetaxel in ABCC1O-overexpressing cells

	$IC_{50} \pm SD^a$ (nmol/L; fold resistance)	
Drugs	**HEK293/pcDNA3.1**	**HEK293/ABCC10**
Paclitaxel	$4.49 \pm 0.43 (1.00)^b$	$66.20 \pm 6.48 (14.74)$
+Ibrutinib 1 μmol/L	$4.07 \pm 0.60 (0.91)$	$21.44 \pm 2.80 (4.78)^c$
+Ibrutinib 2.5 μmol/L	$3.92 \pm 0.77 (0.87)$	$10.95 \pm 0.58 (2.44)^c$
+Ibrutinib 5 μmol/L	$3.81 \pm 0.65 (0.85)$	$4.86 \pm 0.44 (1.08)^c$
+ Cepharanthine 5μmol/L	$3.93 \pm 0.75 (0.88)$	$4.30 \pm 0.46 (0.96)^c$
Docetaxel	$0.93 \pm 0.05 (1.00)^b$	$14.57 \pm 3.10 (15.67)$
+Ibrutinib 1 μmol/L	$0.81 \pm 0.08 (0.87)$	$3.76 \pm 0.56 (4.04)^c$
+Ibrutinib 2.5 μmol/L	$0.78 \pm 0.03 (0.84)$	$1.88 \pm 0.19 (2.02)^c$
+Ibrutinib 5 μmol/L	$0.74 \pm 0.14 (0.80)$	$1.10 \pm 0.13 (1.18)^c$
+Cepharanthine 5 μmol/L	$0.89 \pm 0.10 (0.96)$	$1.09 \pm 0.15 (1.17)^c$
Cisplatin	$1,376.39 \pm 192.89 (1.00)^b$	$1,399.66 \pm 251.62 (1.02)$
+Ibrutinib 1 μmol/L	$1,323.61 \pm 221.12 (0.96)$	$1,449.06 \pm 250.48 (1.05)$
+Ibrutinib 2.5 μmol/L	$1,398.16 \pm 190.22 (1.02)$	$1,596.86 \pm 361.56 (1.16)$
+Ibrutinib 5 μmol/L	$1,297.12 \pm 157.59 (0.94)$	$1,592.87 \pm 191.14 (1.16)$
+Cepharanthine 5 μmol/L	$1,447.57 \pm 236.80 (1.05)$	$1,648.99 \pm 161.26 (1.20)$

NOTE: Cell survival was determined by MTT.

^{a}Values represent $IC_{50} \pm SD$ of at least three independent experiments performed in triplicate.

^{b}The resistance folds (values given in parentheses) were calculated by dividing the IC_{50} values of substrate in HEK293/ABCC10 cells in the absence or presence of inhibitors, or HEK293 cells with inhibitors, by the IC_{50} of the parental cells without reversal agents.

$^c P < 0.05$, significantly different from values obtained in the absence of inhibitor.